Journal of Instrumentation

Design and performance of the front-end electronics of the charged particle detectors of PADME experiment

To cite this article: S. Bertelli *et al* 2024 *JINST* **19** C01051

Published by IOP Publishing for Sissa Medialab

Received: *November 3, 2023*
Accepted: *January 8, 2024*
Published: *January 26, 2024*

Topical Workshop on Electronics for Particle Physics
Geremeas, Sardinia, Italy
1–6 October 2023

Design and performance of the front-end electronics of the charged particle detectors of PADME experiment

S. Bertelli,[b] F. Bossi,[b] S. Ceravolo,[b] G. Corradi,[b] C. Di Giulio,[b] E. Di Meco,[b] K. Dimitrova,[a] R. De Sangro,[b] D. Domenici,[b] A. Frankenthal,[e] F. Ferrarotto,[c] G. Finocchiaro,[b] L.G. Foggetta,[b] M. Garattini,[b] G. Georgiev,[a] P. Gianotti,[b] S. Ivanov,[a,*] Sv. Ivanov,[a] V. Kozhuharov,[a,b] E. Leonardi,[c] E. Long,[c,d] M. Mancini,[b] I. Oceano,[f] F. Oliva,[g] G.C. Organtini,[c,d] G. Piperno,[d] M. Raggi,[c,d] I. Sarra,[b] R. Simeonov,[a] T. Spadaro,[b] E. Spiriti,[b] D. Tagnani,[b] C. Taruggi,[b] E. Vilucchi,[b] P. Valente[c] and A. Variola[c] on behalf of the PADME collaboration

[a] *Sofia University, 5 J. Bourchier Str., Sofia, Bulgaria*
[b] *INFN-LNF, via E. Fermi 54, 00044 Frascati, Italy*
[c] *INFN Sezione di Roma, Roma, Italy*
[d] *Sapienza University, Roma, Italy*
[e] *Princeton University, Princeton, NJ, U.S.A.*
[f] *DESY, Hamburg, Germany*
[g] *Edingburgh University, Edingburgh, U.K.*

E-mail: simo@phys.uni-sofia.bg

Abstract: The PADME experiment at LNF-INFN employs positron-on-target-annihilation to search for new light particles. Crucial parts of the experiment are the charged particle detectors, composed of plastic scintillator bars with light transmitted by wavelength shifting fibers to silicon photomultipliers (SiPMs). The location of the detector — close to a turbomolecular pump, inside a vacuum tank, and exposed to 0.5 T magnetic field — has driven the design of custom modular SiPM front-end and power supply electronics. The design of the system and its performance, confirming the desired sub-ns resolution on the reconstructed particle flying times, is shown and discussed.

Keywords: Front-end electronics for detector readout; Photon detectors for UV, visible and IR photons (solid-state) (PIN diodes, APDs, Si-PMTs, G-APDs, CCDs, EBCCDs, EMCCDs, CMOS imagers, etc); Modular electronics; Timing detectors

*Corresponding author.

https://doi.org/10.1088/1748-0221/19/01/C01051

2024 JINST 19 C01051

Contents

1 Introduction: the PADME experiment and the role and requirements for the charged particle detectors

The gravitational phenomenon of dark matter [1, 2] is yet unsolved by modern physics. A possible explanation is the existence of a hypothetical "Dark Sector", composed of particles interacting with the visible matter only through mediators, weakly coupled to the Standard Model.

The PADME experiment [3] searches for such a mediator, a vector boson [4] A′ (or Dark Photon, DP), detecting the production of an unobservable DP in a $e^+e^- \to \gamma A'$ annihilation reaction by evaluating the missing mass of events with a single photon in the final state [3].

The experiment is taking place at Beam Testing Facility (BTF) of the LNF-INFN. The experiment setup is shown in figure 1, left. Positrons accelerated in the DAΦNE LINAC annihilate on a thin diamond target inside the vacuum chamber, producing γ-rays and potentially the A′. The reaction products are registered by the ECAL calorimeter whose information is used to search for a missing mass, equal to the mass of the DP mediator.

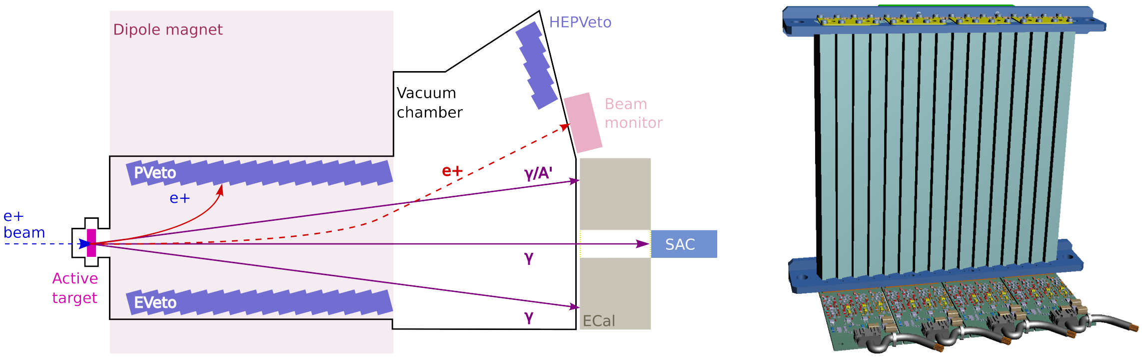

Figure 1. Left: PADME A′ search setup. Right: PADME A′ search charged particle detector, segment.

Charged particles produced in beam-target interactions are deflected onto the E-, the P- and the HEP veto detectors, whose signals are used to reject background events.

2024 JINST 19 C01051

The timing performance of the veto detectors (< 1 ns) and their high efficiency (> 98%) is of key importance. To remove the Bremsstrahlung background, the PADME detector is using a scheme of coincidence between the veto detectors and the small-angle calorimeter (SAC). Also important is the ability to measure the energy of the incident charged particles with resolution better than 5 MeV, which is deduced by the impact point of the particle on the detector, determined by the degree of deflection from a known magnetic field.

The layout of the veto detectors of the PADME A′ search is shown on figure 1, right. The veto detectors are built from polystyrene scintillator rods measuring $10 \times 10 \times 178$ mm^3 with glued-in WLS fiber.

2 Hardware architecture and implementation

The fast organic scintillators are read out by silicon photomultipliers (SiPM). The choice of SiPMs is necessitated by the requirement for operation in a strong magnetic field. Additional benefits of the SiPMs are the small size of the sensor, the low biasing voltages compared to a traditional photomultiplier tube, the high amplification of the SiPM chip, which allowed a simpler analog processing design and the ability to control and monitor the devices with widely available commercial components.

The readout needed to be fast enough to satisfy the requirement for sub-nanosecond time resolution. Due to operation in vacuum, low thermal dissipation, thermal stability, and full remote configurability and control were also required. Figure 2, left, shows the developed device able to satisfy all these requirements.

The Front End Electronics (FEE) system consists of SiPM boards, which are attached to the scintillators and reside in vacuum, and a remote card controller housed in a NIM crate outside the vacuum channel, which outputs the amplified signal to the digital acquisition boards via 50-ohm terminated LEMO connectors and also provides a telnet and http management interface.

Each SiPM board houses 4 SiPM readout channels. A channel (as shown in figure 2, right) is composed of a I^{2}C-controlled voltage regulator, a low-noise, wide bandwidth fast fixed-gain transimpedance preamplifier, a differential output driver and temperature, voltage and current measurement sensors.

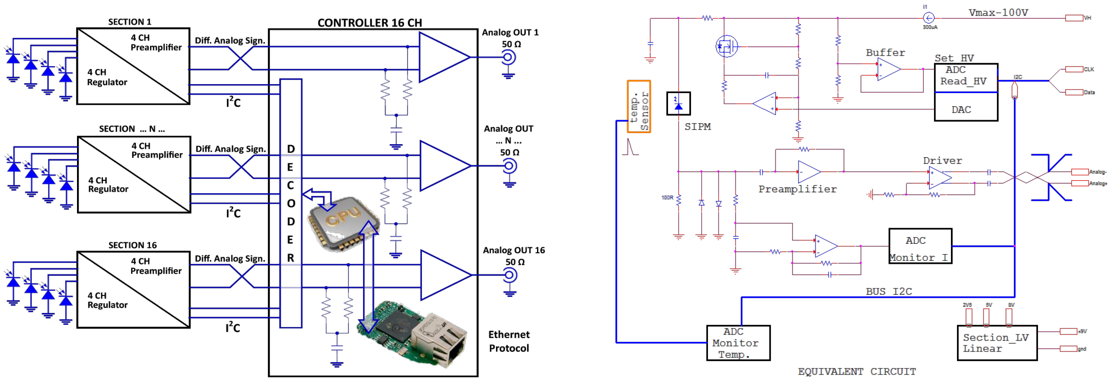

Figure 2. Left: general architecture of the front-end electronics for the charged particle detectors of the PADME Experiment. Right: single SiPM channel architecture.

2024 JINST 19 C01051

The SiPM boards are connected to the external controller via flat twisted pair cables, which carry the generated differential signal to a differential amplifier, and, finally, through the analog output of the controller to the digital acquisition system, which consists of several Caen V1742 switched capacitor digitizer boards [5], recording the voltage output pulse of the FEE.

2.1 Preamplifier and balanced driver

The transimpedance amplifier transforms the current pulse from the SiPM into a voltage pulse that can be recorded by the digital acquisition boards. It is a fixed-gain (gain = 4), single supply amplifier with 70 MHz bandwidth, high repetition rate (> 1 MHz), with pulse resolution better than 10 ns, 1 V output range and low noise with C_{in} 2 pF equivalent of $2\,\mathrm{nV}/\sqrt{\mathrm{Hz}}$.

The balanced driver on the board outputs a differential signal, which is combined on the controller side to avoid noise pick-up from the cables, which go through the vacuum chamber and out to the receiver.

2.2 Biasing

Biasing is implemented with a shunt linear regulator, operating from a 100 V HV supply line from the controller through a current limiter and a regulating power MOSFET. Voltage control is implemented using a DAC-controlled error amplifier, with feedback to the control system provided by an output voltage measurement block on the same board using digital I^2C 2-wire protocol.

The possible adjustment range is from 0 to 95 V, sufficient to drive a large subset of the available SiPM sensors. The device is capable of reading output voltage and setting the output level with accuracy of 16 bits and high ($^1/_{000}$) local feedback stability.

The circuit provides adjustable current protection with a default of I_{max} = 300 µA, the dissipated power at V_{in} = 100 V is 30 mW, and the theoretical thermal stability is 50 ppm, confirmed by simulation. The biasing source has a large rejection ratio of 60 dB to input voltage fluctuations, fast response time to load variation of 100 µs and low noise to the maximum load of 2 mV_{pp}. The biasing circuit can operate from a maximum input voltage of 200 V.

2.3 PCB design and board view

The 4-channel SiPM card is implemented as an 8-layer printed circuit board, with special attention to heat dissipation issues. The SiPM modules are separated from the rest of the electronics with a large isolated heat dissipation area, which is connected to the power ground via large value bridge resistors (figure 3, left).

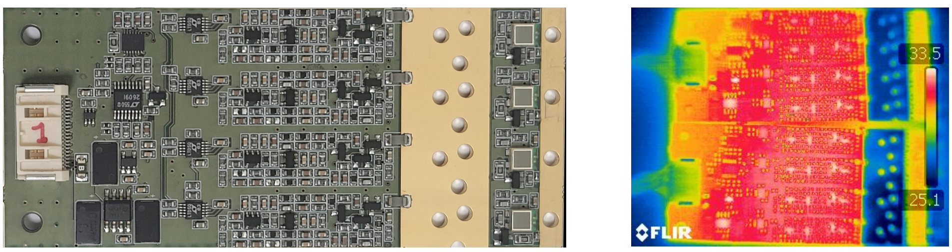

Figure 3. Left: SiPM card photo. Right: SiPM card thermals in operation.

2024 JINST 19 C01051

When in operation (figure 3, right), the SiPMs, are separated from the heat generated by the amplifiers and the biasing circuit, while the bridge resistors allow them to efficiently transfer heat in vacuum. The theoretical maximum power dissipation of a single card with 4 SiPM channels operating is 400 mW.

2.4 Control, data acquisition and triggering

The control system is implemented using an ARM Cortex3 board in a standard NIM chassis. A single controller accommodates up to 16 differential input channels to read out the analog output from 16 SiPMs on 4 boards, and 16 digital I^2C channels for board control and monitoring. Provided are two production end-user interfaces, one over HTTP and one over telnet protocols, and a diagnostic USB interface for device debugging and development. The control interfaces allow both human interaction and full automated remote management by means of integration into a detector control system.

The controller also holds the primary high voltage generator that is used to supply the biasing current, as well as the power supply for the SiPM boards.

The triggering setup for all runs of PADME is implemented on the data acquisition side, where a trigger signal from the LINAC system is distributed to the V1742 boards, and the analog output signal from the SiPM boards is recorded as it arrives from the analog output of the controller.

3 Performance

A SPICE [6] simulation has been developed to validate the operation of the amplifier circuit and to be used for the implementation of digital filters in the reconstruction and analysis processing.

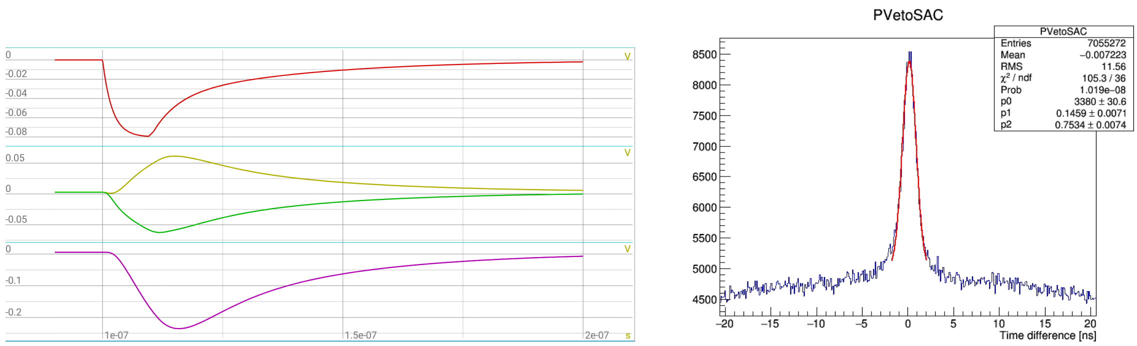

Figure 4. Left: simulated operation of the preamplifier. From top to bottom: input signal, differential output amplified by the SiPM board module, output to digitizer. Right: time resolution of the calibrated veto detector.

The simulation confirms the correct design and operation of the FEE electronics, the temperature stability and the amplitude and frequency response of the amplifier stage, the stability of response of input capacitance and the noise characteristics.

A multi-step procedure has been developed to calibrate the time response of the veto detectors and the time resolution of the veto-SAC operation. The variance of the time response differential between neighboring scintillator rods for the same event was measured for multiple events, establishing a timing calibration curve. Figure 4 right shows the measured time difference with respect to the SAC detector of the PADME experiment confirming a time resolution capability of $\sim$ 750 ps, well under the design requirements of the veto.

2024 JINST 19 C01051

The SiPM cards operation in vacuum underwent extensive testing ahead of the first data-taking run, with measurements of the power dissipation and thermal performance. The measured average power consumption per channel averaged ~125 mW, totalling 12 W per each veto station, consisting of 96 channels. The low power consumption allowed for the use of simple passive cooling setup with a braided copper wire attached from the card to the mounting, resulting in card average temperatures of approximately 8°C above the ambient temperature of the vacuum chamber for the environment temperature range between 20°C ~ 35°C range.

4 Conclusions

A fast, low noise and thermally stable front-end electronics system was developed for the readout of the plastic veto scintillators of the PADME Experiment. It is composed of a controller, located outside of the vacuum chamber, close to the major data acquisition components of PADME experiment, and front-end cards with SiPMs, placed inside the vacuum tank. The controller delivers low voltage, fixed 100 V biasing supply, and communicates through I^2C with the front-end cards to allow bias voltage configuration and SiPM voltage, current, and temperature monitoring. In addition, the controller also provides an ethernet port with web interface to facilitate configuration and monitoring.

The front end card hosts a configurable biasing voltage generator for the SiPMs. To ensure stability, its initial stage is implemented as a current generator, followed by a DAC regulated comparator. The signal from the SiPM is preamplified with a fixed gain of 4 and then output as differential signal, delivering very high immunity against externally induced electromagnetic noise. The differential signals are taken via a feed-through flange and about 10 m long line back to the controller, where they were converted to single ended signal, to match the chosen digitization electronics. A single front-end card serves four independently configurable SiPMs.

The described SiPM front end electronics served more than 200 readout channels for extended periods inside the magnet in vacuum with temperature ranging from 15°C to 46°C, without degradation of its nominal performance.

The whole system has performed well within the requirements for time resolution, power consumption and has excellent thermal and stability characteristics, allowing its successful application in the main and the auxiliary program of the PADME experiment.

Acknowledgments

We warmly thank the BTF and LINAC teams of LNF for providing an excellent quality beam and full support during the data taking period. PADME experiment acknowledges major support from INFN, Italy. Sofia University team acknowledge that partially this study is financed by the European Union-NextGenerationEU, through the National Recovery and Resilience Plan of the Republic of Bulgaria, project SUMMIT BG-RRP-2.004-0008-C01 and TA-LNF as part of STRONG-2020 EU Grant Agreement 824093.

2024 JINST 19 C01051

References

[1] F. Zwicky, *Die Rotverschiebung von extragalaktischen Nebeln*, *Helv. Phys. Acta* **6** (1933) 110.

[2] V.C. Rubin, W.K. Ford Jr. and N. Thonnard, *Extended rotation curves of high-luminosity spiral galaxies. IV. Systematic dynamical properties, Sa → Sc*, *Astrophys. J.* **225** (1978) L107.

[3] M. Raggi and V. Kozhuharov, *Proposal to Search for a Dark Photon in Positron on Target Collisions at DAΦNE Linac*, *Adv. High Energy Phys.* **2014** (2014) 959802 [arXiv:1403.3041].

[4] M. Pospelov, *Secluded* U(1) *below the weak scale*, *Phys. Rev. D* **80** (2009) 095002 [arXiv:0811.1030].

[5] CAEN, *v1742 Switched Capacitor Digitizer*, https://www.caen.it/products/v1742/.

[6] L.W. Nagel and D.O. Pederson, *SPICE (Simulation Program with Integrated Circuit Emphasis)*, Technical Report UCB/ERL M382, EECS Department, University of California, Berkeley (1973), http://www2.eecs.berkeley.edu/Pubs/TechRpts/1973/22871.html.

2024 JINST 19 C01051